Journal of Power Sources 180 (2008) 845–851

Contents lists available at ScienceDirect

Journal of Power Sources

journal homepage: www.elsevier.com/locate/jpowsour

Electrochemical investigation of polarization phenomena and intercalation kinetics of oxidized graphite electrodes coated with evaporated metal layers

F. Nobili, S. Dsoke, M. Mancini, R. Tossici, R. Marassi*

Dipartimento di Scienze Chimiche, Università di Camerino, Via S. Agostino, 1, Camerino 62032, Italy

ARTICLE INFO

Article history:
Received 9 January 2008
Received in revised form 18 February 2008
Accepted 21 February 2008
Available online 29 February 2008

Keywords:
Metal-coated graphite
Electrochemical impedance spectroscopy
Lithium-ion batteries

ABSTRACT

The electrochemical behavior of partially oxidized graphite electrodes coated with 50 Å thick Au, Cu, In, Pb or Sn layers has been studied by slow scan rate cyclic voltammetry and galvanostatic charge–discharge. Electrochemical impedance spectroscopy (EIS) has also been applied to Cu- and Sn-coated electrodes in order to study the effect of the metal coating on the interfacial intercalation/deintercalation kinetics.

The results demonstrate that certain metallic layers produce remarkable improvements of intercalation kinetics of graphite electrodes by reducing the charge-transfer and the solid–electrolyte interface (SEI) resistance making this type of surface modification attractive for the development of high rate anodes for lithium-ion batteries.

1. Introduction

Since its introduction in the late 1980s graphite is the preferential choice as an anode material for lithium-ion batteries because of several reasons mainly related to its relatively high capacity, cyclability and flat charge–discharge profile. Under normal conditions, graphite intercalates reversibly with lithium forming graphite intercalation compounds (GICs) up to LiC_6, with a theoretical capacity of 372 mAh g^{-1}. Substitution of lithium metal with graphite in secondary lithium batteries was mainly due to safety reasons. Lithium metal electrodes suffer of the safety problem caused by dendrite growth causing electrode shorting with production of large amount of heat and gases eventually leading to burning or explosion. However, a stable behavior of graphite anodes requires the presence on its surface of the so-called solid–electrolyte interface (SEI) that is a porous film on the carbon surface that prevents contact of the different stage GICs, formed during intercalation process, with the electrolyte and direct solvent co-intercalation. The latter causes exfoliation of graphite and destruction of its structure. SEI structure and morphology is, therefore, crucial in determining the electrochemical performances of graphite anodes and much attention has been paid in recent years to modifications of the surface structure to favor formation of a low resistance stable SEI. Among the different methods one may mention mild oxidation, deposition of metal and metal oxide layers, coating with polymers or other kind of carbons. A quite recent review [1] deals with surface modification of both anodic and cathodic materials for lithium batteries.

Surface modification may be easily achieved by mild oxidation of native graphite by thermal treatment or wet chemical oxidation [2–15]. Mild oxidation reduces the number of unsaturated carbon atoms at the edge planes (dangling bonds) by forming a dense layer of oxides such as carbonyl, carboxyl and hydroxyl that, after lithiation becomes part of the SEI. Another effect of mild oxidation, either by means of thermal treatment or wet oxidation, is the production of nano-channels and/or micropores that can act as additional host sites for lithium thus improving the overall electrochemical performances. Wet chemical oxidation by means of strong oxidant such as $(NH_4)S_2O_8$, HNO_3, H_2O_2 and $Ce(SO_4)_2$ also remove imperfection such as sp^3 hybridized carbon atoms, carbon chains and carbon radicals increasing stability of the graphite surface and bulk. A considerable amount of work has been devoted to surface modification of graphite electrodes by deposition or coating with metal or metal oxide layers [16–29]. Different metals (Cu, Al, Sn, Pb, Ag, In, Zn, Bi, Pd, Ni, Au) have been used. The presence of a metal layer or metal particles on the surface of the electrodes leads to: (i) a substantial decrease of the charge-transfer and SEI resistance; (ii) an increase of the apparent lithium diffusion coefficient; (iii) an effective protection against solvent co-intercalation and (iv) a general increase in cycling stability.

Although not investigated in details, the nature of the SEI formed on the metal surface is believed to be different from that found on graphite. The charge-transfer is believed to occur on the metal surface. This step is followed by diffusion of lithium into the bulk

* Corresponding author. Tel.: +39 0737 402 214; fax: +39 0737 402 296.
E-mail address: roberto.marassi@unicam.it (R. Marassi).

0378-7753/$ – see front matter © 2008 Elsevier B.V. All rights reserved.
doi:10.1016/j.jpowsour.2008.02.069

graphite and stage formation. Strong evidences have been presented demonstrating that when the metal is able to form alloys (Au, Pb, Ag, Sn, etc.) the intercalation of lithium into graphite occurs through alloy formation [30]. The situation is less clear in the case of copper layers because this metal is not known to form alloys with lithium at least at room temperature. In spite of this, Cu covered graphite electrodes readily intercalate lithium and the metal layer is very effective in preventing the decomposition of propylene carbonate and exfoliation of graphite caused by co-intercalation of solvated lithium ions [29]. In addition, it has been demonstrated that lithium ions can migrate (diffuse) through compact 30 μm thick Cu metal foil [21] placed in a bipolar cell in which one side of the copper foil was polarized at 10 mV vs. Li in a $LiClO_4$ containing EC/DMC solution while the other side was poised at +3 V vs. Li in a $NaClO_4$ containing the same solvent. The mass transfer of un-solvated Li^+ is believed to occur in the vacant space not occupied by copper ions in the copper lattice probably assisted by phonon-briefing phenomena. The copper film, besides not obstructing lithium migration, seems to play an active catalytic role as a mediator of the charge-transfer process.

In this context, this paper deals with electrochemical behavior and characterization of composite electrodes made of graphite, partially oxidized by thermal treatment, coated by thin evaporated metallic layers of Au, Cu, In, Pb or Sn. The paper follows a recent one [31] in which the electrochemical behavior of graphite/nano-size metal composites (Au, Ag, Ni, Cu, Al, Sn) in the temperature range 20 to −30 °C has been described. The main purpose is to investigate, by means of different electrochemical techniques, the role played by the metal layers in improving the overall intercalation/deintercalation kinetics.

2. Experimental

Timrex KS-15 graphite (Timcall, specific area 12 $m^2\,g^{-1}$, average particle size 7.7 μm, interlayer distance 3.36 Å) oxidation was carried out in air at 750 °C for 45 min. Before thermal treatment, the graphite samples were dried under vacuum overnight at 200 °C. The oxidation degree was roughly estimated by the weight loss (about 30%) and by the oxygen content (about 11%) determined from elemental analysis data [31].

The electrodes were then manufactured by preparing a slurry of oxidized graphite, carbon (Super-P, MMM Carbon), PVdF (Aldrich) and oxalic acid (Carlo Erba) in NM2P with the following composition: graphite:carbon:PVdF:$H_2C_2O_4$ 84.5:5:10:0.5 w/o. The inks were then coated onto electrolytic copper (12.5 μm by Schlenk) using the "doctor blade" technique and dried at 120 °C under vacuum. The loading of the electrodes (0.64 cm^2 surface area) was of the order of 1.5–2 mg cm^{-2} of active mass. Metallic coatings were prepared by metal evaporation in a vacuum chamber, using tungsten crucibles to hold the pure metals (Au, Cu, Sn, Pb and In). The metals were allowed to evaporate onto the carbon surface kept at room temperature by applying suitable currents to the crucible. Deposit thickness was controlled by monitoring the weight of electrodes with a quartz crystal microbalance. The experimental conditions were adjusted in order to obtain layers with thicknesses in the range 50–150 Å.

The measurements were performed using T-shaped polypropylene Swagelok type cells equipped with stainless steel (SS304) current collectors. Disks of high-purity lithium foil by Foote Mineral Co. were used as counter and reference electrodes. A polypropylene film (Cellgard 2400, Celanese Co.) was used as separator. The electrolyte was a 1 M solution of $LiPF_6$ in EC:DEC:DMC 1:1:1 (LP71 by Merck). The cells were assembled in a dry-box and cycled three times at a charge–discharge rate of C/3 in order to form a homogeneous solid–electrolyte interface. After the first three cycles, the cells were opened in order to remove any possible gases developed during SEI formation, sealed again and brought out of the box for the electrochemical characterization. All the electrochemical measurements have been made using a VMP2/Z galvanostat–potentiostat by PAR Instruments (Oak Ridge, TN). EIS spectra have been recorded over the frequency range 100 kHz to 1 mHz at selected potential values in the range 250–50 mV during the intercalation process using a perturbation of 5 mV. Before each measurement the electrodes were equilibrated at the selected potentials for 3–5 h. The electrode morphology was investigated by SEM using a Cambridge Stereoscan 360. All the experiments were run at room temperature.

3. Results and discussion

3.1. Morphology

Fig. 1 shows SEM micrographs of an oxidized graphite electrode (Fig. 1a) and of electrodes coated with 50 Å Cu (Fig. 1b) and Sn (Fig. 1d) layers. The micrographs reveal that the metals cover uniformly the electrode surface. This is confirmed also by the backscattered electrons images (Figs. 1c and d) that are consistent with the presence of a homogeneous and continuous metallic film without macroscopic fractures. The micrographs of electrodes covered by other metals (not shown for sake of brevity) are quite similar to the ones shown revealing that compact metal layers can be easily formed on graphite electrodes by vacuum deposition.

3.2. Galvanostatic measurements

Fig. 2 shows first three galvanostatic charge–discharge profiles at C/3 rate for the pristine and the metal modified electrodes. The shapes of the first intercalation curves demonstrate that a SEI is formed at each electrode over a potential range ranging from about 0.8 to 0.5 V vs. Li before the usual plateaus below 0.3 V characteristic of lithium staging into graphite. No other process, beside SEI formation, is observed involving alloy formation or reduction of oxides either on the galvanostatic curves or on the corresponding differential capacity curves dq/dE (not shown for sake of brevity). This may be due to the low quantity of metal present on the sample surface that prevents the observation of plateaus (or peaks on the dq/dE curves) due to, for instance, alloy formation at Sn, Pb, In and Au that are known to form alloys of different stoichiometry at room temperature upon electrochemical intercalation of Lithium in non-aqueous electrolytes containing lithium salts [21,30]. If the deposited metals are partially oxidized during electrodes preparation and handling, some evidences for irreversible reactions involving oxide reduction in the potential range 0.9–1.5 V should also be observed [32–35] but, again, if indeed present, the quantity of oxide is probably too low to give detectable evidences on the electrochemical curve. The irreversible capacities are of the order of 30–40% of the theoretical capacity for all electrodes. The lowest values (around 20%) are found for the un-modified and the In covered electrodes. This suggests that SEI formation on the metal covered electrodes follows different-additional paths with respect to the unmodified graphite.

Apart from the uncertainty in determination of exact loadings, reversible capacities at second cycle are similar for all the electrodes and close to theoretical value of 372 mAh g^{-1}. In addition, as shown in Fig. 3, the electrodes show excellent capacity retention upon cycling with only minor losses after 50 cycles of continuous cycling at C/5 rate. Breaking/reformation phenomena of passivation layer are the probable reason of the occasional spikes observed in capacity values in the case of the uncoated and Pb-coated elec-

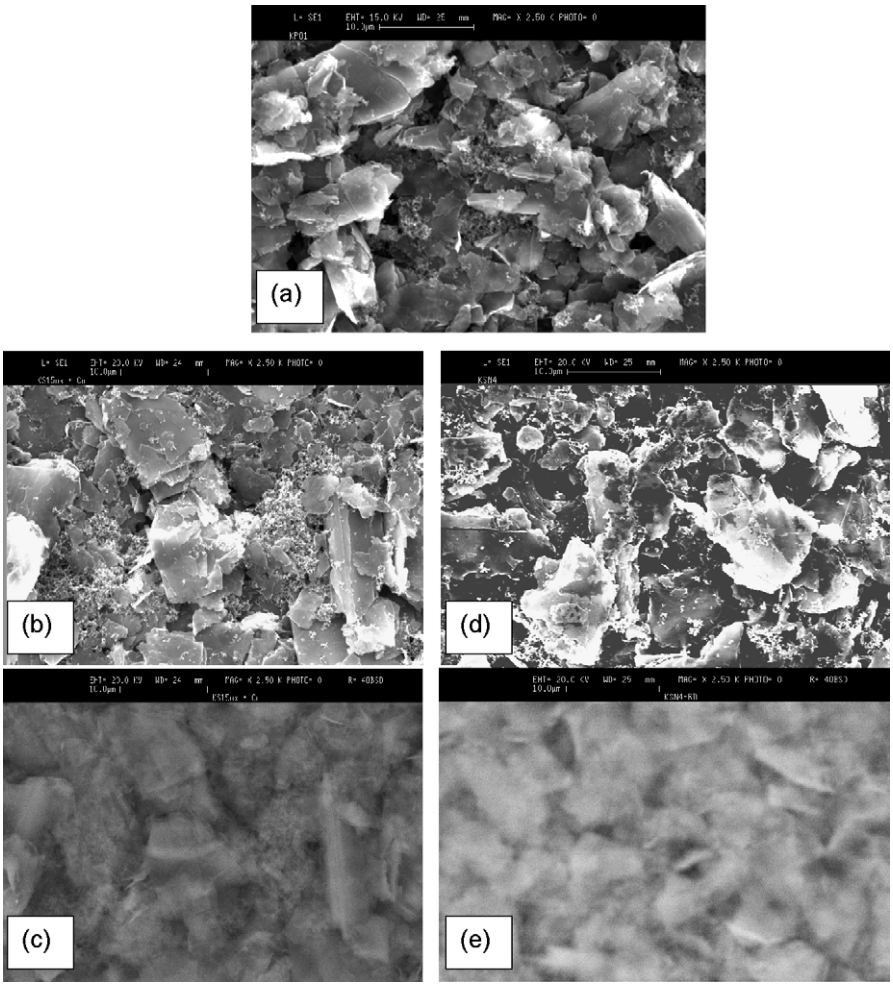

Fig. 1. SEM micrographs of pristine (a) Cu-coated (b) and Sn-coated (d) electrodes, (c) and (e) backscattered electrons images of (b) and (d).

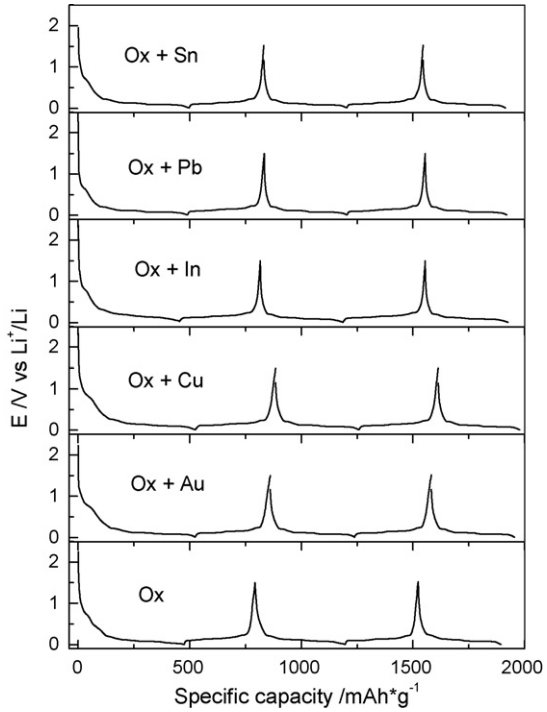

Fig. 2. Galvanostatic intercalation/deintercalation profiles of electrodes coated by 50 Å layers of various metals: Au, Cu, In, Pb, Sn and pristine electrodes at C/3 rate.

trodes. The best result, either in terms of cyclability and reversible capacity, is observed at In covered electrodes suggesting an excellent stability of the SEI. The worst electrode is the Au-coated that retains only about 80% of the initial capacity after 50 cycles. This results is consistent with previous results obtained with Au covered graphitized carbon fiber electrodes in which the poor cyclability of the electrodes was attributed to formation of inadequate SEI and/or collapse of the film due to alloy formation [16,21,39].

All these findings suggest that the very thin metallic coatings (50 Å) do not significantly contribute to the electrode capacity and that at least part of the metal is involved in the formation of the passivation layer. The formed SEI, even if results in a relatively large irreversible capacity, is effective in stabilizing the electrode/electrolyte interface.

3.3. Cyclic voltammetry

Slow scan rate cyclic voltammetry (SSCV) has been used in order to evaluate the effect of the metal coating on the intercalation mechanism. Fig. 4 shows the voltammograms obtained at a scan rate of 10 $\mu V\,s^{-1}$ in the potential range 0.005–0.3 V vs. Li^+/Li at 20 °C using the pristine electrode and electrodes coated with 50 Å thick Au, Cu, Sn, In and Pb layers. The electrodes were previously cycled at least three times at C/3 rate in order to form a stable SEI. The cut-off potentials are limited to the region of Li staging in graphite since, as explained in the previous section, no other important pro-

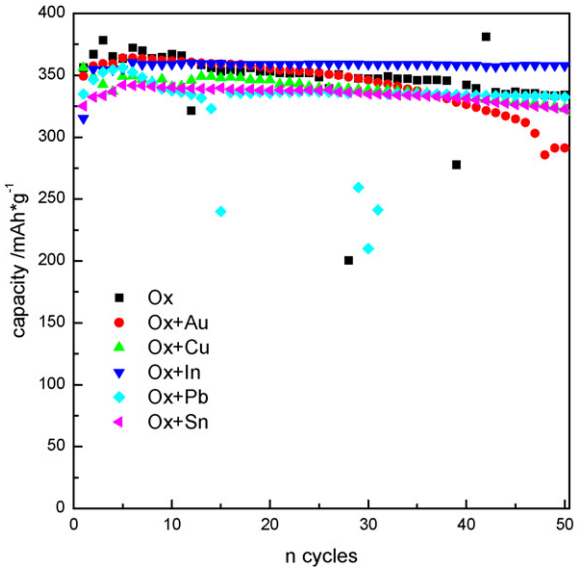

Fig. 3. Deintercalation capacities vs. cycle number for the different electrodes at C/5 rate.

cess appears to be operative at higher potential values. In order to directly compare the results, all the current values are normalized to the active mass. The general shape of the cyclic voltammograms of all the electrodes is the one expected for natural graphite. Based on the literature data, the three main processes associated with the wave-couples E/F, D/C and A/B (as marked for the Cu-coated electrode) corresponds to two-phase regions LiC_6/LiC_{12}, LiC_{12}/LiC_{27} and LiC_{36}/LiC_{72}. In natural graphite the reversible potentials of these three couples are known to be equal to 85, 120 and 210 mV, respectively [36,37]. The midpoint potentials between the anodic and cathodic peaks for the three main processes are within few mV equal the above values for all electrodes demonstrating that partial oxidation and surface layers do not modify the lithium staging processes. At the scan rate of 10 $\mu V\,s^{-1}$ the cycling voltammograms are equivalent to a coulometry and, hence, by integrating the current one may obtain information on the faradic efficiency. In addition, as the currents are normalized to the weight of the active material, the intercalation/deintercalation capacities should be equal for all electrodes. Again the data demonstrate that, the modifications introduced by the oxidation and by the metal deposits do not appreciably affect the intercalation mechanism. Within the uncertainty in the determination of the effective weight of the active material, the intercalation capacity is the same for all electrodes and close to the theoretical value of 372 mAh g^{-1}. However, as shown by the shape of the cyclic voltammograms, the kinetics of the intercalation/deintercalation processes depends on the type of surface modification. The peaks relative of the three main processes are higher and sharper in the case of Au, Sn, Pb and Cu covered electrodes suggesting faster overall electrode kinetics and phase transitions compared with that of "naked" or In covered electrodes. The result for the In modified electrodes appears to be in contradiction with those obtained in the cyclability test. The reasons are at present not very clear and deserve further investigation involving the nature of the SEI and its relation with the irreversible capacity that, in the case of In, is the lowest among those of the metal modified electrodes.

Fig. 5 shows cyclic voltammograms obtained with electrodes coated with 50, 100 and 150 Å thick Cu layers. As it may be seen the peaks become progressively lower and less sharp with increasing thickness. At the same time the integrated charge during the intercalation steps change from 370 to 320 and 310 mAh g^{-1} for the 50, 100 and 150 Å layers, respectively. These results suggest that, while effective in improving the overall kinetics of intercalation/deintercalation steps, the metal layer, at least in the case of copper, affects the overall capacity probably acting as a physical barrier towards Li^+ transport. The decrease in capacity with increasing film thickness is consistent with the results of Suzuki et al. [30] who measured the amount of lithium intercalated in Cu covered graphitized carbon fiber electrodes through the height of the deintercalation peak in cyclic voltammetric curves obtained at 1 mV s^{-1}

3.4. EIS measurements

Following the indications of Levi and Aurbach [37] the intercalation of lithium into graphite may be thought as a sequence

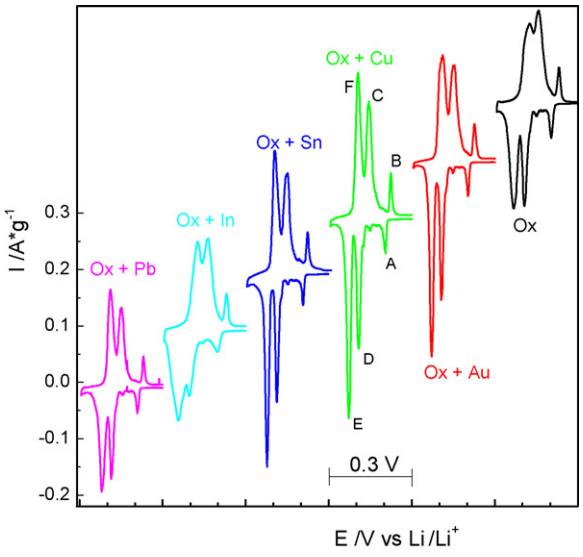

Fig. 4. Cyclic voltammograms of electrodes coated by 50 Å layers of various metals recorded at scan rate = 10 $\mu V\,s^{-1}$ and T = 20 °C. The curves are shifted of 0.3 V along the potential axis and of 0.1 A g^{-1} along the current axis.

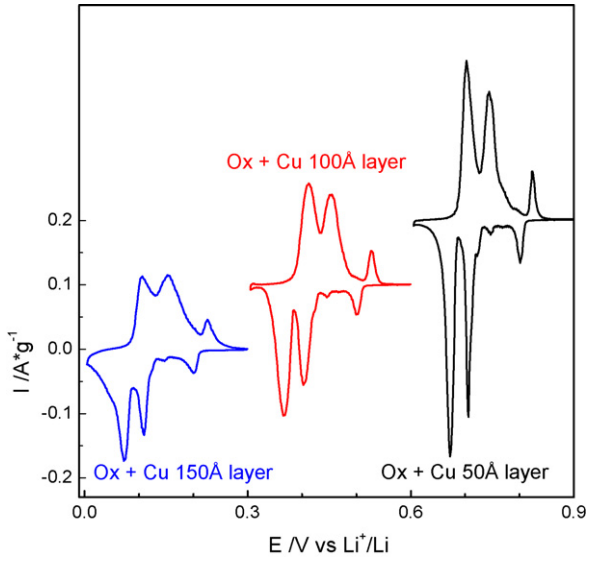

Fig. 5. Cyclic voltammograms of electrodes coated by Cu layers of various thicknesses recorded at scan rate = 10 $\mu V\,s^{-1}$ and T = 20 °C. The curves have been shifted of 0.3 V along the potential axis and of 0.1 A g^{-1} along the current axis.

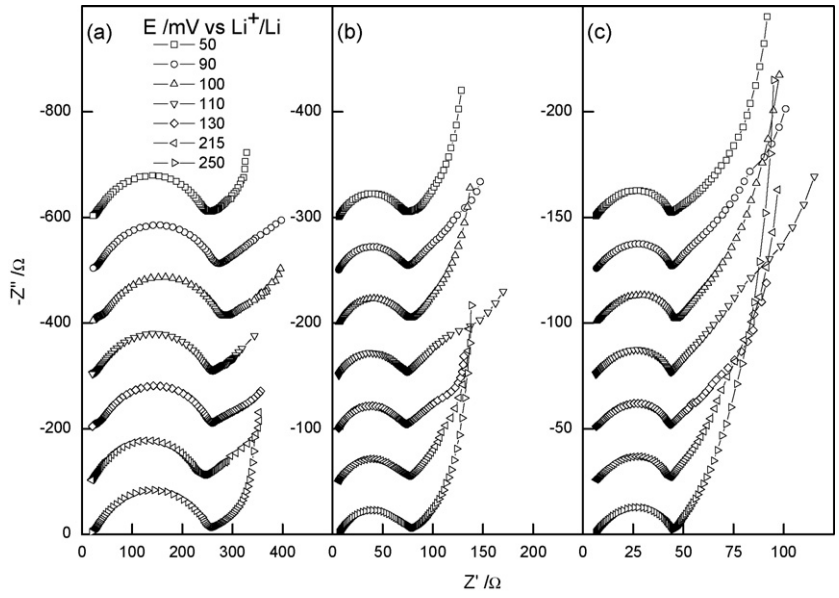

Fig. 6. Nyquist plots at some significant potentials for: (a) uncoated electrode; (b) electrode coated with Cu; (c) electrode coated with Sn.

of several processes occurring in series: ion conduction in solution, diffusion of ions in solution at the interface, migration of Li ions through the surface film, charge-transfer, solid-state diffusion and accumulation–consumption of Li into the bulk. At the scan rate used in the cyclic voltammetric experiments and for the electrodes used in this study (thin electrodes using the Levi criteria [37]), the current response is under thermodynamic control and reflects the accumulation–consumption absorption-type behavior rather than diffusion or charge-transfer processes. In the present case, the presence of the metal layer, with all the implications relative to transport of lithium through the layer, adds a further complication in the interpretation of the electrochemical results. The problem has been addressed using EIS and taking into account that all the studies relative to metal modified graphite electrodes are in agreement in indicating that the effect of the metal is reflected by a decrease of the charge-transfer resistance and hence by an increase of the overall intercalation kinetics. Sn and Cu have been chosen because of their good voltammetric behavior, high reversible capacity, good cycle life and, in addition, because they may be considered as representative of alloy and no-alloy forming metals. Unmodified electrodes have been studied as well for comparison. Fig. 6 shows a series of impedance dispersion for the pristine (panel a), Cu- (panel b) and Sn- (panel c) coated electrodes taken at different potentials. The impedance dispersions are directly comparable as the graphite loadings of the different electrode are the same and, as suggested by Levi and Aurbach [37,38] the mass ratio can be used as scaling factor when the electrodes have similar geometry. As a general observation it may be pointed out that, at any potential, the overall impedance of the metal covered electrodes is much lower than that of the pristine electrode in agreement with the literature findings.

All the impedance dispersions show: (i) a typical slightly depressed semicircle in the middle-frequency region that is generally attributed can to a charge-transfer; (ii) a more or less defined semicircle at higher frequencies, that partly overlaps the first one, that may be attributed to Li^+ migration through the surface layer; (iii) a 45° dispersion in the low-frequency region that typically describes diffusion; (iv) at some of the potentials a vertical line in the low-frequency limit that reflects the blocking character of the intercalation capacity.

The vertical line, that describes a blocking behavior, is easily detected at 50 and 250 mV vs. Li^+/Li, practically corresponding to fully intercalated or deintercalated electrodes. The dispersions of the electrodes coated by Cu or Sn layers show an additional, more or less defined arc in the low-frequency region, where signature of solid-state diffusion is expected, as a peculiar feature. The arc is more defined at potentials where staging transitions occur. Fig. 7 shows the dispersions at 0.11 V vs. Li for the three electrodes on a larger scale. As may be seen the arc is more developed at Cu than at Sn-coated electrodes and is completely absent in the pristine electrode. Deviations from an ideal 45° line characteristic of Warburg type diffusion, with formation of arcs or semicircles in Nyquist plots at low-frequency, have been discussed by several authors. Relevant to the present case are the papers by Levi and Aurbach [38,39] that attribute the low-frequency arc to the exis-

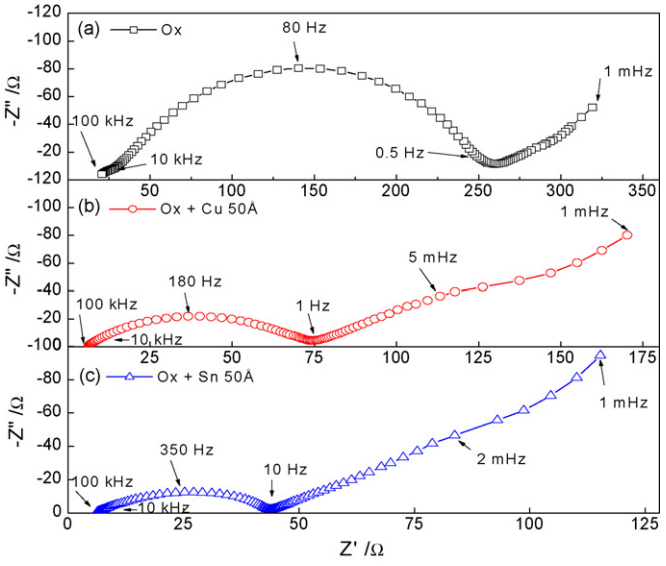

Fig. 7. Enlarger view of Nyquist plots at 0.11 V vs. Li for: (a) uncoated electrode; (b) and (c) Cu- and Sn-coated electrodes.

tence of diffusive processes with different time constants resulting for instance from regions of the electrode having different thickness. The existence of different time constants for diffusion is very likely in the present case as, if the metal layers are compact as it seems, Li^+ has to diffuse through the layer, with or without alloy formation, before being incorporated into graphite. As the layer is very thin, the resulting diffusion should be the one expected for a finite length Warburg-diffusion at a non-blocking interface as described by a cotangent-hyperbolic function (circuit element O) according to Boukamp notation [40].

The presence of the metal layer, and the fact that lithium ions have to diffuse through it before being incorporated into graphite, has other implications on the intercalation mechanism. Before crossing the copper layer, or as a consequence of alloy formation on tin, solvated lithium ions in solution must lose their solvation sheath. The rate of solvation/desolvation has been recently recognized as the rate determining step of the charge-transfer process [41–45] based on the evidences that the charge-transfer resistance depends on the solvent composition and that the activation energy for the so-called charge-transfer is of the order of 50–70 kJ mol^{-1}. Values in this range are believed to be the typical intercalation energy barriers for breaking up the Li^+ solvation sheath. To further support to this way of thinking, it has been observed [41–45] that, in intercalation electrodes, either anodes or cathodes, the real charge-transfer occurs between the active material, graphite or transition metal oxide, and the electron sink/reservoir (current collector) with a process that does not involve Li^+ diffusion and reduction. Hence, the term charge-transfer in the classical meaning of electron exchange between an electrode and an incoming ion is not applicable in the case of intercalation electrodes. This concept is hardly new as it was applied by Bruce and Saidi [46] to explain the mechanism of intercalation with the so-called adatom model in which Li^+ ions are thought to be adsorbed onto the electrode surface after loosing their solvation sheath. At the same time electrons enter the host lattice to preserve electroneutrality and the lithium ions are accommodated into the lattice. The same model has been recently applied to explain the EIS spectra of intercalation cathodes [47–49].

Attempts to simulate the entire dispersions using a serial or parallel combination of finite space and finite length diffusion elements [38] or the adatom equivalent circuit [46–49] were not entirely satisfactory especially in the low-frequency region. The two different arcs are probably too overlapped to be satisfactory discriminated. Variations of physical parameters, such as temperature and/or layer thickness, that may results in a better separation of the different features, are at present under investigation. In spite of this, some conclusions can be drawn by limiting the analysis of the spectra to the medium frequency region including the well developed semicircle, attributed to the so called charge-transfer, using a conventional equivalent circuit such as, in Boukamp notation [40], $R_e(R_{SEI}Q_{SEI})(R_{ct}Q_{dl})$ (where R_e is the uncompensated electrolyte resistance, R_{SEI} and R_{ct} are the SEI and the charge-transfer resistances and Q_{SEI} and Q_{dl} are the associated capacities that have been simulated using the constant phase element Q to take into account the depressed nature of the semicircles). The relevant values of R_{SEI} and R_{ct} for the three electrodes are plotted in Fig. 8 as a function of the potential (i.e. degree of intercalation). As it may be seen the calculated R_{ct} values for all electrodes are practically invariant with the potential. This is consistent with the adatom model in which the rate-limiting step of intercalation is formation of the adatom and its desolvation (either on the SEI or the combined SEI–metal surface) rather than direct electron transfer to incoming Li^+ ions [46] that leads to a typical Butler–Volmer dependence of R_{ct} on potential. Preliminary results [50] obtained with Cu-coated electrodes seem to confirm this type of conclusion as the activation energy for

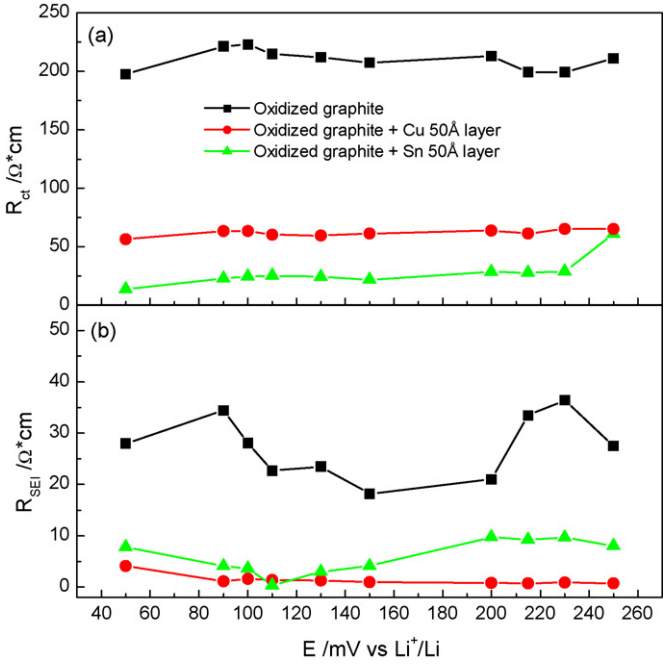

Fig. 8. Trends of charge-transfer resistance R_{ct} (a) and of passivation layer resistance R_{SEI} (b) as a function of the potential for the uncoated electrode and for the electrodes coated by Cu and Sn layers.

charge-transfer is around 50 kJ mol^{-1} as expected if the rate determining step is the Li^+ desolvation rate. The values of charge-transfer resistances of the electrodes coated by Cu or Sn are almost one order of magnitude lower than those of the "naked" one. Sn, in addition, appears to be more effective than Cu in reducing the charge-transfer resistance suggesting that alloy formation is more effective that a physical barrier, such as the one exerted by copper, in improving the intercalation kinetics. The actual mechanism is, however, still not completely understood but the indications obtained with the EIS measurements are in agreement with the improvement in voltammetric behavior previously observed for the coated electrodes. This confirms that the metal layers are able to improve the exchange kinetics at graphite electrodes thus pointing towards a catalytic role of the metals in increasing the charge-transfer rate. This is in agreement with Huang et al., who assigned such a catalytic role to some transition metals, either as oxide or in metallic state [35] suggesting an increase in electronic conductivity at electrode surface and an enhancement of desolvation rate as possible paths for the decrease of activation barrier of the overall intercalation process. An additional effect of the metallic layers is a decrease of the resistance of passivation layer. This is probably due to the incorporation of a small amount of metal that increase its bulk conductivity or, more likely, to the formation of an additional or alternative phase over the metallic coatings as suggested by the observed increase in irreversible capacity at first cycle.

4. Conclusions

The modification of oxidized graphite electrodes by coating with relatively thin evaporated metal layers, especially Cu and Sn, is effective in enhancing electrochemical performances of anodes, by improving the charge-transfer rate through a mechanism that involves a different and/or less resistive SEI and an increased Li^+ desolvation rate. Further work is at present in progress to clarify the nature of the SEI and of the additional arc at low frequency that is present in the impedance dispersion of the coated electrodes.

Acknowledgement

This work was supported by MIU, PRIN 2005.

References

[1] L.J. Fu, H. Liu, C. Li, Y.P. Wu, E. Rahm, R. Holze, H.Q. Wu, Solid State Sci. 8 (2006) 113.
[2] E. Peled, C. Menachem, D. Bar-Tow, A. Melman, J. Electrochem. Soc. 143 (1996) L4.
[3] M.E. Spahr, H. Wilhelm, F. Joho, J. Panits, J. Wambach, P. Novak, N. Dupont-Pavlosky, J. Electrochem. Soc. 149 (2002) A960.
[4] Y.P. Yu, C. Wan, C. Jiang, S.B. Fang, Y.T. Jang, Carbon 37 (1999) 1901.
[5] N.A. Asrian, G.N. Bondarenko, G.I. Yemelianova, L. Gorlenko, A. Liubov'Ye, O.I. Adrov, R. Marassi, V.A. Nalimova, D.E. Sklovsky, Mol. Cryst. Liquid Cryst. 340 (2000) 331.
[6] C. Menachem, Y. Wang, J. Flowers, E. Peled, S.G. Greenbaum, J. Power Sources 76 (1998) 180.
[7] C. Menachem, E. Peled, L. Burstein, Y. Rosenberg, J. Power Sources 68 (1997) 277.
[8] X. Cao, J.H. Kim, S.M. Oh, Electrochim. Acta 47 (2002) 4085.
[9] Y.P. Wu, C.Y. Jiang, C. Wan, R. Holze, Solid State Ionics 156 (2003) 283.
[10] Y.P. Wu, C.Y. Jiang, C.R. Wan, E. Tsuchida, Elecrochem. Commun. 2 (2002) 272.
[11] Y. Ein-Eli, V.R. Koch, J. Electrochem. Soc. 144 (1997) 2968.
[12] Y.P. Wu, C.Y. Jiang, C. Wan, R. Holze, J. Appl. Electrochem. 32 (2002) 1011.
[13] Y.P. Wu, C.Y. Jiang, C. Wan, R. Holze, J. Power Sources 111 (2002) 329.
[14] Y.P. Wu, C.Y. Jiang, C. Wan, R. Holze, Electrochem. Commun. 4 (2002) 483.
[15] Y.P. Wu, C.Y. Jiang, C. Wan, E. Tsuchida, J. Mater. Chem. 11 (2001) 1233.
[16] T. Takamura, J. Suzuki, C. Yamada, K. Sumiya, K. Sekine, Surf. Eng. 15 (1999) 225.
[17] P. Yu, J.A. Ritter, R.E. White, B.N. Popov, J. Electrochem. Soc. 147 (2000) 2081.
[18] J.Y. Lee, R. Zhang, Z. Liu, J. Power Sources 90 (2000) 70.
[19] P. Yu, J.A. Ritter, R.E. White, B.N. Popov, J. Electrochem. Soc. 147 (2000) 1280.
[20] B. Veeraraghavan, A. Duraviajan, B. Haran, B. Popov, R. Guidotti, J. Electrochem. Soc. 149 (2002) A675.
[21] T. Takamura, K. Sumiya, J. Suzuki, C. Yamada, K. Sekine, J. Power Sources 81–82 (1999) 368.
[22] J. Suzuki, M. Yoshida, C. Nakahara, K. Sekine, M. Kikuchi, T. Takamura, Electrochem. Solid State Lett. 4 (2001) A1.
[23] L. Shi, Q. Wang, H. Li, Z. Wang, X. Huang, L. Chen, J. Power Sources 102 (2001) 60.
[24] Y.P. Wu, C. Wan, C. Jiang, L. Li, Z. Wang, Chin. J. Power Sources 23 (1999) 191.
[25] H. Mamose, H. Hombo, S. Takeuchi, T. Horiba, M. Oda,. Koseki, Y. Muranka, Y. Kozono, J. Power Sources 68 (1997) 208.
[26] K. Nishimura, H. Hombo, S. Takeuchi, T. Horiba, M. Oda, M. Koseki, Y. Muranaka, Y. Kozono, H. Miyadaera, J. Power Sources 68 (1997) 436.
[27] S. Kim, Y. Kadoma, H. Ikuta, Y. Uchimoto, M. Wakihara, Electrochem. Solid State Lett. 4 (2001) A109.
[28] J. Gao, H.P. Zhang, L.J. Fu, T. Zhang, Y.P. Wu, T. Takamura, H.Q. Wu, R. Holze, Electrochim. Acta 52 (2007) 5417.
[29] J. Gao, L.J. Fu, H.P. Zhang, T. Zhang, Y.P. Wu, H.Q. Wu, Electrochem. Commun. 8 (2006) 1726.
[30] J. Suzuki, M. Yoshida, Y. Nishijima, K. Sekine, T. Takamura, Electrochim. Acta 47 (2002) 3881.
[31] F. Nobili, S. Dsoke, T. Mecozzi, R. Marassi, Electrochim. Acta 51 (2005) 536.
[32] F. Belliard, Solid State Ionics 135 (2000) 163.
[33] J. Santos-Peña, Solid State Ionics 135 (2000) 87.
[34] S.H. Ng, J. Electrochem. Soc. 153 (2000) A787.
[35] H. Huang, E.M. Kelder, J. Schonman, J. Power Sources 97–98 (2001) 114.
[36] T. Ohzuku, Y. Iwakoshi, K. Sawai, J. Electrochem. Soc. 140 (1993) 2490.
[37] M.D. Levi, D. Aurbach, J. Electroanal. Chem. 421 (1997) 79.
[38] M.D. Levi, D. Aurbach, J. Phys. Chem. B 101 (1997) 4630.
[39] M.D. Levi, D. Aurbach, J. Phys. Chem. B 108 (2004) 11693.
[40] B.A. Boukamp, Solid State Ionics 20 (1986) 159.
[41] T. Abe, H. Fukuda, Y. Iriyama, Z. Ogumi, J. Electrochem. Soc. 151 (2004) A1120.
[42] T. Abe, M. Ohtsuka, F. Sagane, Y. Iriyama, Z. Ogumi, J. Electrochem. Soc. 151 (2004) A1950.
[43] T. Abe, F. Sagane, M. Ohtsuka, Y. Iriyama, Z. Ogumi, J. Electrochem. Soc. 152 (2005) A2151.
[44] K. Xu, J. Electrochem. Soc. 154 (2007) A162.
[45] K. Xu, Y. Lam, S.S. Zhang, T.R. Jow, T.B. Curtis, J. Phys. Chem. B 111 (2007) 7411.
[46] P.G. Bruce, M.Y. Saidi, J. Electroanal. Chem. 322 (1992) 93.
[47] F. Nobili, R. Tossici, R. Marassi, F. Croce, B. Scrosati, J. Phys. Chem. B 106 (2002) 3909.
[48] F. Nobili, S. Dsoke, M. Minicucci, F. Croce, R. Marassi, J. Phys. Chem. B 110 (2006).
[49] F. Nobili, S. Dsoke, F. Croce, R. Marassi, Electrochim. Acta 50 (2005) 2307.
[50] F. Nobili, S. Dsoke, M. Mancini, R. Marassi, in preparation.